



Published in final edited form as:

ACS Appl Mater Interfaces. 2019 October 09; 11(40): 36324–36332. doi:10.1021/acsami.9b11095.

Phospholipid-Coated Hydrophobic Mesoporous Silica Nanoparticles Enhance Thrombectomy by High Intensity Focused Ultrasound with Low Production of Embolism-Inducing Clot Debris

Nicholas T. Blum, Ciara M. Gyorkos[‡], Spencer J. Narowitz[‡], Evan N. Mueller, Andrew P. Goodwin^{*}

Department of Chemical and Biological Engineering, University of Colorado Boulder, Boulder, Colorado 80303, United States

Abstract

Here we report the efficacy of a nanoparticle-assisted high intensity focused ultrasound (HIFU) treatment that selectively destroys blood clots while minimizing generation of microparticles, or microemboli, that can cause further complications post-surgery. Treatment of malignant blood clots (thrombi) and the resulting emboli are critical problems for numerous patients, and treatments addressing these conditions would benefit from advancements in noninvasive procedures such as HIFU. While recanalization of occlusive blood clots is currently addressed with surgical intervention that seeks to minimize formation of large emboli, there is a danger of microemboli (micron-size particles) that have been theorized to be responsible for the poor correlation between apparent surgical success and patient outcome. Here, the addition of phospholipid-coated hydrophobically modified silica nanoparticles (P@hMSNs) improved the efficacy of HIFU treatment by serving as cavitation nuclei for mechanical disruption of thrombi. This treatment was evaluated for the ability to clear the HIFU focal area of a thick and dense thrombus within 10 min. Moreover, it was found that the use of P@hMSN+HIFU treatment generated a significantly smaller microembolic load as compared to comparison techniques, including HIFU + microbubble contrast agent, HIFU alone, and direct mechanical disruption. This reduction in the microembolic load can occur either with primary removal of the clot by P@hMSN+HIFU or by insonation of the clot fragments after mechanical thrombectomy. Lastly, this method was evaluated in a flow model, where non-occlusive model thrombi and model emboli were mechanically ablated within the focal area within 15 s. Together, these results represent a

^{*} **Corresponding Author:** andrew.goodwin@colorado.edu.

Author Contributions

The manuscript was written through contributions of all authors. All authors have given approval to the final version of the manuscript.

[‡]These authors contributed equally.

ASSOCIATED CONTENT

Supporting Information.

The following files are available free of charge.

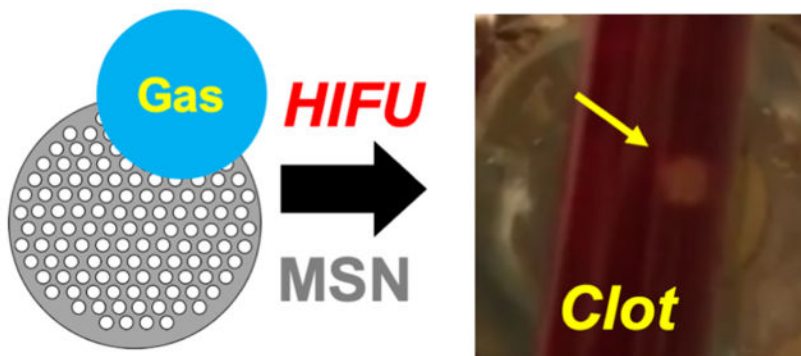
Supplemental figures showing calibrations for mass determination of blood removed, full distributions from supernatants of treated clots with FLOWCAM, and confirmation of acoustic activity via ultrasonic analysis (PDF)

Mechanical ablation of a smooth, flat clot with HIFU after injection of nanoparticles (MOV)

Lack of mechanical ablation with HIFU before the injection of nanoparticles (MOV)

combination therapy capable of resolving thrombi and microembolisms resulting from thrombectomy through localized destruction of clotted material.

Graphical Abstract



Keywords

Thrombosis; atherosclerosis; nanoparticle; ultrasound; cavitation

Introduction

Cardiovascular disease is responsible for nearly half of non-communicable disease mortality around the world.¹ A major contributor to this mortality is the prevalence of thrombosis, which has increased with the increased incidence of chronic vascular disease, particularly in developed countries.² Thrombosis in its most common form occurs when patients suffering from atherosclerosis, an underlying chronic inflammatory condition, have sufficient plaque build-up in their arteries. If the plaques rupture, clots can form on the ruptured plaque within the artery, rapidly occluding the vessel.^{3,4} Thus, a chronic cardiovascular condition can rapidly progress into an acute coronary infarction or stroke if the clot occludes an artery feeding the heart or brain, respectively. Similarly, venous thrombosis can lead to acute thromboembolism, and when this results in a pulmonary embolism the prognosis is poor.⁵⁻⁷ Tools and procedures for treating a thrombotic lesion should also reduce the risk of embolization for improving recurrence, hospitalization, and patient survival outcomes.⁸⁻¹³ The main preventative techniques for reducing risk of embolization during clot thrombolysis are concurrent aspiration, aortic filtration, and thrombectomy with stent,¹⁴⁻¹⁷ followed by infusion of heparin.

Even with these treatments and precautions, however, only small correlations have been observed between apparent surgical success and patient outcome.^{9,10} Shortfalls in patient outcome may be explained by the generation of microemboli, or micron-size particles that may occlude or damage smaller vessels but escape detection in patients.¹⁸⁻²² There is compelling evidence that large amounts of microembolic particles, defined here as a macroparticle with diameter $>3 \mu\text{m}$ but much smaller than the diameter of a typical embolus,^{23,24} have significant negative effects on post-operative cognition in both animals and humans, potentially due to occlusion of blood vessels in the brain.²⁵⁻²⁷ The impact of a high

microembolic load can be patient-specific,²⁴ there is still debate as to whether or not microembolic load is critical for long-term patient survival, and the mechanism by which microemboli generate adverse effects is unknown. However, there is consensus in the medical community that treatment techniques should be evaluated for their ability to minimize microembolic load.^{28,29}

In this work, we utilize high intensity focused ultrasound (HIFU) to reduce both embolic and microembolic load. HIFU has been shown by several groups to be an effective tool for selectively destroying both thrombi and emboli in animal models.^{30–36} Treatments with HIFU are both non-invasive and associated with high recanalization rates,^{31–33} and microemboli may be reduced by using pulsed, cavitation-inducing waveforms.^{37,38} Adding ultrasound contrast agents to circulation can improve the efficacy of HIFU, especially with repeated HIFU exposures,^{39–43} which is important given the long exposure times typically associated with HIFU standalone treatments, particularly when treating large volumes.⁴⁴ Microbubbles have been the primary choice for enhancing HIFU thrombolysis, and several formulations are FDA-approved contrast agents. However, microbubbles come with significant disadvantages, including their short half-life in vivo, high primary acoustic scattering that defocuses the HIFU beam, and an inability to perfuse through dense environments such as a blood clot.^{43,45,46}

In order to address several of these limitations, our group has created phospholipid-capped, hydrophobically modified silica nanoparticles (P@hMSNs) that are capable of generating mechanical cavitation events without significant temperature rise.^{47,48} We have shown in previous work that the P@hMSNs nucleate air pockets stabilized by defects on the lipid surface. These air pockets are stabilized by a combination of the hydrophobic silica modification, the surface roughness caused by the mesoporous structure, and an amphiphilic coating that decreases the interfacial tension at the bubble-water interface (Figure 1A).⁴⁹ Here, in order to stabilize the hydrophobic MSN surfaces in biological media, phospholipids were chosen because they are generally recognized as safe, their properties have been extensively characterized, and their packing is favorable for the assembly of monolayers and bilayers, particularly those that are supported by silica.^{50–52} Following nucleation, the bubble nuclei are converted to large, transient microbubbles by HIFU pulses (Figure 1A). These produced microbubbles scatter ultrasound waves and then collapse, generating shockwaves and additional collapsing bubbles that cause mechanical damage to their surroundings.^{49,53,54}

Here, we show that P@hMSNs sensitize the application of HIFU for thrombolysis and outperform microbubbles in terms of enhancement of the therapeutic effect. The proposed mechanism by which the combination therapy of P@hMSNs and HIFU can assist in the breakdown of a thrombus *in vitro* are shown in Figure 1 for both the static and flow models. Briefly, without P@hMSNs, HIFU waves pass through the clot without causing damage, as the intensities and duty cycle are insufficient to cause significant temperature rise (see below). However, the P@hMSNs are able to capture the HIFU energy to promote cavitation events on the nanoparticle surface, resulting in focused mechanical damage to the clot in the focal region. In this work, we show that this method can clear channels through occlusive clots in both static and flow models. Beyond showing complete destruction of a thrombus in

the HIFU focal zone in as little as 15 s in a flow model, destruction of clots using P@hMSNs produced far fewer microemboli than both direct mechanical thrombectomy and other HIFU treatments. We also show that this microembolic matter was converted to “nano-embolic” matter, which should be harmless as it shares many compositional similarities as nanoscale drug delivery vehicles and naturally forming fibrin protofibrils.^{55–57} Thus, P@hMSNs represent a type of contrast agent that can destroy occlusive blood clots safely and completely with minimal risk of post-procedure side effects.

Materials and Methods

Materials:

Calf whole blood in sodium citrate was purchased from Lampire Biological Laboratories. Deionized (DI) water was obtained by filtering distilled water through a Milli-Q Advantage A10 system (MilliporeSigma, Inc.) and was used without degassing. Phosphate buffer saline (PBS, 1X), cetyltrimethylammonium chloride (CTAC, 25 wt.% in water), Triton-X100, concentrated HCl, ethanol, hexanes, dichloromethane (DCM), and chloroform were purchased from Sigma. Tetraethylorthosilicate (TEOS) was purchased from Acros Organics. Triethylamine (TEA), calcium chloride, and perfluorobutane (PFB) were purchased from Alfa Aesar. Dodecyltrichlorosilane (DDTS) was purchased from Gelest Inc. 1,2-dipalmitoyl-sn-glycero-3-phosphocholine (DPPC), 1,2-distearoyl-sn-glycero-3-phospho-ethanolamine-N-[methoxy(polyethylene glycol)-2000] (DSPE-PEG2k), and 1,2-distearoyl-sn-glycero-3-phospho-ethanolamine-N-[methoxy(polyethylene glycol)-5000] (DSPE-PEG5k) were purchased from Avanti Polar Lipids Inc.

Synthesis of Mesoporous Silica Nanoparticles (MSNs):

This procedure was adapted from previous publications.^{49,53,54} In a 50 mL round bottomed flask, 15 mL of DI water and 5 mL of CTAC were added. The mixture was stirred in a water bath for 30 min at ~600 rpm and 75 °C with a condenser attached to the flask. Then, 0.8 mL of an aqueous TEA solution (10 v/v% in DI water) was added and the reaction vessel was stirred at 80 °C for 45 min. Afterwards, 1.5 mL TEOS was added dropwise and the mixture stirred at 80 °C for another 90 min. The resulting milky white suspension was centrifuged at 7100 rcf for 30 min and washed once with ethanol. The supernatant was decanted off, and the particles were resuspended in acidic ethanol (12.5 mL conc. HCl in 1 L ethanol), then stirred in a bath at 65 °C with condenser for 2 h. This was repeated once before washing with ethanol three times and placing back in a bath at 65 °C to allow the nanoparticles to dry overnight before storing in a plastic centrifuge tube at RT.

Synthesis of Hydrophobically Modified MSNs (hMSNs):

This procedure was adapted from previous publications with some modifications.^{49,53,54} 25 mg of MSNs were crushed into a fine powder with a mortar and pestle and placed in an oven at 120°C for 20 min. The particles were allowed to cool to RT, then dispersed in 25 mL of anhydrous DCM and placed in a bath to stir at 600 rpm at RT under argon. 600 µL of DDTS was added and allowed to react for 24 h in a round bottomed flask covered with a glass stopper. The suspension was then washed two times with hexanes and once with ethanol, centrifuged at 7100 rcf for 30 min, then dried overnight in a 65 °C bath. The resulting

contact angle of the particles when spread evenly on a glass slide was approximately 140°, indicating that the hydrophobic modification had been successful (Figure S1).

Phospholipid Coating and Aqueous Suspension of hMSNs (P@hMSNs):

This procedure was adapted from previous publications.^{49,53,54} 4.4 mg of hMSNs were baked in an oven at 120°C for 90 min and then allowed to cool to RT. The dried hMSNs were then suspended in 1 mL of chloroform and bath sonicated for 4 min. 500 µL of 4 mg mL⁻¹ DPPC in chloroform and 300 µL of 2 mg mL⁻¹ DSPE-PEG2k in chloroform were added, and the solution was bath sonicated for 3 min. The mixture was dried, uncapped, on a water bath at 75 °C. After 90 min, 2 mL of DI water was added along with a stir bar, capped, placed back in the bath at 75 °C and stirred for 45 min at ~600 rpm. The solution was then centrifuged at 10,000 rcf for 5 min. The nanoparticles were washed twice and split into 4 2-mL centrifuge tubes, where they were stored as a pellet with the supernatant removed at RT.

Transmission Electron Microscopy (TEM):

TEM images of the nanoparticles were taken using a T12 Spirit (FEI Tecnai) microscope. TEM samples were prepped by dispersing the lipid-coated hydrophobically modified particles in 1% uranyl acetate aqueous solution and then drying them onto a carbon TEM grid.

Contact Angle Measurements:

5 mg of an aqueous slurry of hMSNs were placed onto a glass slide and kept in an oven at 85°C for 30 min. The particles were pushed into one location on the slide with a spatula, another glass slide was placed on top, and the two slides were squeezed together by hand to form a flat surface. The top slide was removed, and a spatula was used to brush off any loose particles. Finally, the static contact angle of a sessile water droplet on the film was measured on a ramé-hart Model 210 Goniometer/Tensiometer.

Synthesis and Size Fractionation of Microbubbles:

2 mL chloroform was added to 8 mg of DPPC (1,2-dipalmitoyl-sn-glycero-3-phosphocholine) and bath sonicated until dispersed. The solution was dried on a rotary evaporator at RT for 40 min. 2 mL PBS was added and the mixture was rotated, without vacuum, at 55 °C for 7 min. Then the bath temperature was increased to 75 °C and the flask was rotated for 20 min. After this process, 250 µL of the lipid suspension was combined with 720 µL of PBS and 74 µL of a 4.2 mg mL⁻¹ DSPE-PEG5k solution in water and transferred into a 2 mL centrifuge tube. PFB gas was then bubbled through the lipids/PBS solution until the solution and headspace were saturated. To make microbubbles, the tip of a probe sonicator (Branson SLPe 1/4" diameter tip) was placed at the liquid-gas interface, and the suspension sonicated for 10 s at 70% amplitude. During sonication, the probe tip was moved slowly to align with the liquid-gas interface as bubbles formed.

To fractionate the microbubbles, the sample was centrifuged for 3 min at 300 rcf. The supernatant was removed and replaced with 1 mL PBS. This wash step was repeated once more. Then, the solution was taken up in a 1 mL syringe and allowed to rest inverted (tip upwards) in the syringe for 10 min to allow the larger bubbles to float to the top. The top 0.4

mL of the solution was discarded, and the rest was stored in a glass vial with PFB re-filled into the headspace.

Blood Clot Formation:

The tip of a 3 mL plastic transfer pipette (Fisherbrand) was cut off and the bulb section kept. 0.1 mL of calf whole blood was mixed with 3 μ L of a 1 M aqueous calcium chloride solution and placed in the bulb of the pipette. The blood was allowed to clot overnight at the bottom of the bulb (opening upwards) in a humidity chamber held at 95% relative humidity at RT.

Mechanical Thrombectomy:

In order to simulate a mechanical thrombectomy, a metal spatula was scraped through the clot repeatedly for 1 min with the intent to disrupt and break down the thrombus as much as possible.

HIFU Setup and Conditions:

HIFU was generated using a single element HIFU transducer (Sonic Concepts H101, 64.0 mm Active Diameter x 63.2 mm Radius of Curvature) with a coupling cone (Sonic Concepts C101). The transducer cone was filled with degassed and deionized water and then submerged in a water tank. The HIFU transducer was connected to a Waveform Generator (Agilent Technologies) using an AG Series Amplifier (T&C Power Conversion, Inc.) operating at 100% output. The following Waveform Generator settings were used: 800 mVpp, 1 MHz frequency, 10 ms burst period, and 12 cycles. These settings correspond to a peak negative pressure of about 10 MPa and a duty cycle of about 0.11%.⁵⁴

Clot Treatment with High Intensity Focused Ultrasound:

In a typical experiment, to the blood clot in the transfer pipette was added either 200 μ g of P@hMSNs in 1 mL PBS, 4 μ L of the microbubble suspension diluted into 1 mL PBS, or 1 mL PBS. The bulb of the inverted pipette was placed on top of the coupling cone. HIFU was then applied for 5 min.

Determination of Mass Loss from Disrupted Blood Clot:

In order to measure the amount of disrupted mass in the supernatant of the blood clot, the supernatant was collected and then lysed with the addition of a 10% Triton X-100 solution to a final Triton concentration of 0.1%. The clot/Triton mixture was mixed for 1 h on a shaker plate at 37°C and 600 rpm. The resulting solution was transferred to a 96-well plate and the hemoglobin absorbance was measured at 540 nm, which was then converted to a mass via a calibration curve (Figure S2).

Size Characterization of Particles in Supernatant Post-Treatment:

For size detection of blood clot remnants after thrombi destruction, the supernatant was removed after the blood clots were exposed to each treatment (P@hMSNs+HIFU, HIFU only, mechanical thrombectomy, and microbubbles + HIFU) using a glass pipette. A ProteinSimple MFI 5000 Bot 1 was used for size characterization of the microemboli

generated from the clot disruption. The MFI Bot is a form of flow imaging microscopy in which the sample flows via a Fluid Imaging Technologies FlowCAM VS instrument in front of a 10x brightfield objective within a 100 μL flow cell. Bright field images are then captured and analyzed for particulate matter within a range of 2–100 μm size equivalent circular diameter.

Measurement of Temperature Rise during HIFU Insonation:

A PBS sample with or without P@hMSN was subjected to the HIFU conditions described above. During the measurement, the temperature was recorded by a thermocouple placed inside the sample but outside the HIFU focus. Temperature was recorded every 30 s for a total of 15 min for each sample, done in triplicate.

Flow Model Setup:

The flow model was created by using a Fisherbrand Variable-Flow Peristaltic pump connected via Tygon tubing to the cylindrical portion of a 3 mL Falcon disposable pipette that had the bulb and tapered dispenser cut off. The clot was pre-formed in the disposable pipette stem in the same manner and conditions as the inverted pipette experiments. The flow was $\sim 5\text{--}10\text{ mL min}^{-1}$, and 1 mg mL^{-1} particles were added via injection into the Tygon tubing during HIFU insonation.

Statistical Tests:

The Mann-Whitney U Test was conducted for statistical significance between conditions. The Mann-Whitney U Test determines whether it is reasonable that the two results come from the same distribution and does not require an assumption of normality. Thus, the null hypothesis is that the two results or conditions come from the same distribution and the alternative is that they come from different distributions. It is specified in the text whether the test was one-sided or two-sided, and the alpha value for significance was 0.05.

Results & Discussion

P@hMSNs were synthesized as described in previous publications,^{49,53,54} and both the porosity and hydrophobicity were confirmed by TEM (Figure 1) and static contact angle measurements (140° , Figure S1), respectively. Next, we tested the effect of P@hMSN-sensitized HIFU on a 100 μL simulated thrombus. After forming the clot, a 1 mL suspension of the contrast agent (P@hMSN, microbubble, or none) in PBS was placed above the thrombus (Figure 2A), followed by application of HIFU for 10 min. To simulate thrombectomy, 1 mL PBS was placed on top of the thrombus, followed by 1 min of mechanical disruption with a metal spatula with the intent to break up the clot as much as possible. When HIFU (10.8 MPa peak negative pressure, 10 ms pulse repetition frequency, 12 waveforms per pulse) was applied without contrast agent, little damage was observed (Figure 2B). The addition of a 10 μL bolus of concentrated microbubble suspension ($\sim 10^9\text{ mL}^{-1}$) enhanced observable damage as compared to the HIFU-only treatment, with some visible lightening in the clot. In comparison, addition of $100\text{ }\mu\text{g mL}^{-1}$ P@hMSNs significantly increased the effectiveness of HIFU in breakdown of the thrombus, with a hole formed in the center of the thrombus. The $\sim 3\text{ mm}$ diameter hole is similar to the estimated

HIFU focal diameter of 2.5 mm. As expected, mechanical disruption (thrombectomy control) led to significant clot breakage, but the damage was highly non-uniform. It is also important to note that the clot pieces post-thrombectomy were loose and only remained stuck to the container surface by adsorption; such large, loose clot pieces would be especially dangerous for a patient. In comparison, the clots treated with P@hMSN-enhanced HIFU remained fixed in position, as there was little change to areas outside the HIFU focus. It should also be noted that this procedure resulted in a small temperature rise, $< 3\text{ }^{\circ}\text{C}$, over the course of insonation, whether P@hMSNs had been added or not (Figure S3). It should also be noted that this measurement was conducted inside a static water bath; in circulation the body would be expected to dissipate heat more rapidly due to blood circulation and interstitial fluid convection. Thus, the destruction of the clot can be concluded to arise from mechanical rather than thermal effects.

The amount of blood removed from the clot was quantified by analyzing the hemoglobin content of the supernatant by its UV-Vis absorbance. The post-treatment supernatant was removed from the samples and Triton X-100 was added to a final concentration of 1 mg mL^{-1} , which was necessary to reduce variations in absorbance values due to light scattering by particulates in the supernatant.⁵⁸ After shaking the suspension for 1 h at 37°C , the absorbance was measured on a plate reader at 540 nm, which corresponds to oxygenated hemoglobin absorbance.⁵⁹ The hemoglobin absorbance values were then correlated to the mass of blood through a constructed calibration curve (Figure S2). By applying this calibration to the absorbance values for the lysed supernatants of the clots, the mass of blood removed from a clot can be accurately estimated (Figure 2C). A small amount of blood, about 4 mg of a $\sim 100\text{ mg}$ clot, was removed from the thrombus during simple pipetting, incubation, and agitation from moving the phantom from preparation area to treatment setup and then back again. In comparison, application of 10 min HIFU insonation without contrast agent led to the release of an insignificant amount of additional blood ($\sim 5\text{ mg}$ total). With the addition of $10\text{ }\mu\text{L}$ of a concentrated microbubble solution giving a final concentration of approximately 2×10^7 microbubbles per mL, the amount of mass removed was marginally greater, increasing to $\sim 8\text{ mg}$, but such levels of removal are likely to be clinically insignificant. However, when a thrombus was treated with HIFU plus P@hMSNs, the amount of mass removed was significantly greater, approximately $\sim 26\text{ mg}$, not significantly different than the values obtained for a mechanical thrombectomy model ($\sim 27\text{ mg}$, two-sided $p\text{-value}=0.885$). This value is consistent with a HIFU focal region of 2.5 mm diameter with 5 mm clot depth. The presence of nanoparticles or microbubble debris scattering contributed negligible amounts of apparent absorbance (Figure S4). Thus, it is clear that P@hMSN-enhanced HIFU is able to lyse significant amounts of material from a thrombus and all of the material within the focal volume of the transducer. The P@hMSNs, when exposed to HIFU, generate large transient bubbles which collapse in inertial cavitation, creating shockwaves and high shear forces capable of breaking down the blood clot. Without nanoparticles, the HIFU pulses used in this study are not powerful enough to generate inertial cavitation events, so they are unable to provide any physical force with which to generate a therapeutic effect.

Having shown that P@hMSNs could improve HIFU-mediated thrombolysis while reducing large, free-floating debris, their effect on clot removal was then studied in more detail. First,

the time of HIFU insonation was varied (Figure 3A), and the amount of material released from the clot was measured as described in the previous experiment. For the first 10 min of HIFU insonation, there was a monotonically increasing trend in the amount of blood released from the clot into the supernatant, followed by a leveling with no significant changes in blood removal from the thrombus. However, after 10 min, cavitation was still occurring, as shown by ultrasound imaging of bubbles formed from HIFU interaction with the P@hMSNs (Figure S5). The lack of additional blood release with continued cavitation is likely because at this time point the clot has been removed completely from the focal zone of the HIFU, which in turn is consistent with the expected clot removal calculation as described above. This trend was observed again when determining the effect of P@hMSN concentration on thrombolysis. As mass of particles added to the 1 mL supernatant increased for a constant 10 min HIFU exposure, mass was removed from the blood clot with an apparent monotonic trend until $100 \mu\text{g mL}^{-1}$, at which point no more mass could be removed from the clot (Figure 3B). While the removed mass appears to decrease slightly as particle concentration is increased to $200 \mu\text{g mL}^{-1}$, the difference in clot removal between the results at $100 \mu\text{g mL}^{-1}$ and $200 \mu\text{g mL}^{-1}$ was not statistically significant (one-sided p-value=0.188) and may be attributed to the overall heterogeneity of clot structure. Thus, while clot removal increases with P@hMSN loading, ultimately only clot mass in the focal zone is affected.

As discussed in the Introduction, one of the goals of this work was to evaluate the P@hMSNs' potential for minimizing microembolic material released from the clot. To measure microparticle count, the amounts of microemboli released into the supernatant from each treatment condition were evaluated by FLOWCAM analysis post-treatment, which works by identifying 2–100 μm sized particles via brightfield imaging of a small-volume flow cell. Since larger microemboli than smaller microparticles, the counts were separated into two bins (>3 and $>20 \mu\text{m}$) to represent the approximate diameters of red blood cells and capillaries, respectively. Interestingly, the number of $>3 \mu\text{m}$ microemboli generated from P@hMSN+HIFU thrombolysis is similar to those generated from HIFU alone, at just ~ 2000 microemboli per mL, even though a far greater clot mass was removed by exposure P@hMSNs (one-sided p-value=0.015). Clots treated with microbubbles and HIFU also exhibited low numbers of microemboli as compared to the thrombectomy model (100,000s of microemboli per mL), but still generate $>3x$ more microemboli (~ 7000 per mL) than from P@hMSN-sensitized treatment (Figure 4). The contribution from the buffer itself was minimal (Figure S6). This reduction in particle count for P@hMSNs was seen across all size bins in this region, so the effect appears to be universal across all microparticle sizes rather than a conversion of larger particles to smaller particles.

We theorized that nanoparticle-assisted HIFU destruction of a thrombus simultaneously breaks down parts of the clot as it is removed from the thrombus. This effect is similar to those observed in our previous work that showed lysis of cancer cell spheroids.⁴⁷ If so, there should be more nanoparticulate matter to account for the increased clot mass removal (Figure 2). This supposition was supported by Nanoparticle Tracking Analysis measurements of the submicron particle concentration (Figure 4B). The control treatment (no HIFU) and HIFU only generated a minimal number of sub-micron particulates, and MB +HIFU and thrombectomy possessed a greater amount. However, the submicron particle

count generated from clots treated with P@hMSN + HIFU produced almost an order of magnitude more nanoparticles than any other treatment. Because these lipid particulates can be safely removed from the blood by the liver and/or spleen, it appears that P@hMSNs can greatly reduce the number of particles capable of producing dangerous microembolic matter.

Similarly, these nanoparticles could be utilized after thrombectomy treatment as a method to reduce the microembolic load and reduce patient stress. The samples first were subjected to mechanical thrombectomy as described before, then either HIFU alone, HIFU + 10 μ L suspension of microbubbles, or HIFU + 100 μ g of P@hMSNs (Figure 4C). The results show that HIFU alone scarcely reduces the amount of microembolic matter as compared to measurement post-thrombectomy alone (Figure S7). The microembolic load for all sizes was effectively reduced post-treatment with the addition of the microbubble solution by about 50% of HIFU alone. However, with the application of HIFU + nanoparticles, the microembolic load is reduced to less than 5% for all size bins. This result shows that HIFU + nanoparticle assisted therapy can be utilized effectively as a post-thrombectomy treatment to reduce microembolic load after more conventional clot-destroying therapies.

Finally, we validated the capabilities of P@hMSN-assisted HIFU thrombolysis in a flow model. First, a thrombus was formed in a plastic tube connected to a peristaltic pump. The thrombus was then placed over the HIFU focus during flow and was exposed to HIFU waves for a minimum of 15 s. If no P@hMSN was added, no change was observed in the thrombus (Figure 5A). After injection of 1 mg P@hMSNs and 15 s HIFU, clot dissolution was observed in the HIFU focal zone. An additional section of the clot could be easily removed by simply shifting the clot position relative to the HIFU transducer and applying another 15 s of HIFU (Figure 5B). In another example, a more globular and occlusive clot was formed, and ~60 s HIFU without P@hMSNs produced no change in clot position or structure (Figure 5C). After administration of P@hMSN and 15 s HIFU insonation, the clot was destroyed almost completely. It should be noted that the reduced time relative to the pipette bulb experiments (Figures 1 and 2) was caused by the smaller clot diameter in the flow model; the model pipette tube has an internal diameter of 5 mm, which is fairly representative of major arteries in the human body.⁶⁰ This effectively demonstrates that HIFU and P@hMSNs can be effectively used in combination for rapid, effective thrombolysis with a reduction in the likelihood of adverse outcomes by reducing the generation of micron-sized embolic matter.

Conclusion

In this work, we have demonstrated the utility of using phospholipid-coated hydrophobically-modified mesoporous silica nanoparticles (P@hMSNs) to enhance high intensity focused ultrasound (HIFU) for reliable and repeated lysis of thrombus models in vitro. In terms of clot mass removal, this method matches or exceeds competing therapies such as mechanical thrombectomy or HIFU with microbubble contrast agent. Moreover, effective therapy can be achieved within minutes for large and dense thrombi and seconds in a smaller flow model. Perhaps most importantly, the micro-embolic load generated by the HIFU + P@hMSN therapy is much lower than those of competing therapies, with micron particle counts similar to those found without any clot treatment. Through both microparticle

and nanoparticle characterization, it appears that the cavitation events from the nanoparticles aid in breaking the dangerous microscale embolic particles down to nanoscale sizes that should not have significant adverse clinical effects. It was also demonstrated that the HIFU + hMSN therapy can be used in a post-mechanical thrombectomy setting with high embolic matter to reduce the microembolic load and with it the risk of a major embolism. Finally, the efficacy of P@hMSNs for enhancing HIFU treatment was verified in an *in vitro* flow model, which showed the recanalization of blood clots in seconds, thereby showcasing the rapid therapeutic potential of these nanoparticles.

Supplementary Material

Refer to Web version on PubMed Central for supplementary material.

ACKNOWLEDGMENT

The authors thank NIH (DP2EB020401 and R21EB026006) for support of this research. The authors would like to thank Prof. Ted Randolph, Austin Daniels, and Hao Wu for training and use of the FLOWCAM, as well as helpful discussions. We acknowledge Dr. Sanli Movafaghi for help with obtaining contact angle measurements. Finally, we also acknowledge Profs. Jennifer Cha, Al Weimer, and Dmitri Simberg for helpful suggestions.

ABBREVIATIONS

MSNs	Mesoporous silica nanoparticles
hMSNs	hydrophobically-modified mesoporous silica nanoparticles
P@hMSNs	phospholipid-coated hydrophobic mesoporous silica nanoparticles
HIFU	high intensity focused ultrasound
MB	microbubble
NP	nanoparticle
DI	deionized
PBS	phosphate buffer saline
CTAC	cetyltrimethylammonium chloride
DCM	dichloromethane
TEOS	tetraethylorthosilicate
TEA	triethylamine
DDTS	dodecyltrichlorosilane
DPPC	1,2-dipalmitoyl-sn-glycero-3-phosphocholine
DSPE-PEG2k	1,2-distearoyl-sn-glycero-3-phospho-ethanolamine-N-[methoxy(polyethylene glycol)-2000]

DSPE-PEG5k	1,2-distearoyl-sn-glycero-3-phospho-ethanolamine-N-[methoxy(polyethylene glycol)-5000]
PFB	perfluorobutane

REFERENCES

- (1). WHO. Global Status Report on Noncommunicable Diseases 2014. WHO Press: Geneva, 2014.
- (2). Jackson SP Arterial Thrombosis—Insidious, Unpredictable and Deadly. *Nat. Med.* 2011, 17, 1423–1436. [PubMed: 22064432]
- (3). Libby P Inflammation in Atherosclerosis. *Arterioscler., Thromb., Vasc. Biol.* 2012, 32, 2045–2051. [PubMed: 22895665]
- (4). Burke AP; Kolodgie FD; Farb A; Weber DK; Malcom GT; Smialek J; Virmani R. Healed Plaque Ruptures and Sudden Coronary Death. *Circulation* 2001, 103, 934–940. [PubMed: 11181466]
- (5). Kearon C Natural History of Venous Thromboembolism. *Circulation* 2003, 107, I22–I30. [PubMed: 12814982]
- (6). Church V Staying on Guard for DVT and PE. *Nursing* 2000, 30, 34–42.
- (7). Ramzi DW; Leeper KV DVT and Pulmonary Embolism: Part II. Treatment and Prevention. *Am. Fam. Physician* 2004, 69, 2841–2848. [PubMed: 15222649]
- (8). Henriques JPS; Zijlstra F; Ottervanger JP; de Boer M-J; van 't Hof AWJ; Hoorntje JCA; Suryapranata H Incidence and Clinical Significance of Distal Embolization during Primary Angioplasty for Acute Myocardial Infarction. *Eur. Heart J.* 2002, 23, 1112–1117. [PubMed: 12090749]
- (9). Chueh J-Y; Puri AS; Wakhloo AK; Gounis MJ Risk of Distal Embolization with Stent Retriever Thrombectomy and ADAPT. *J. Neurointerv. Surg.* 2016, 8, 197–202. [PubMed: 25540180]
- (10). Ito H No-Reflow Phenomenon and Prognosis in Patients with Acute Myocardial Infarction. *Nat. Rev. Cardiol.* 2006, 3, 499–506.
- (11). Gosk-Bierska I; Wysokinski W; Brown RD; Karnicki K; Grill D; Wiste H; Wysokinska E; McBane RD Cerebral Venous Sinus Thrombosis: Incidence of Venous Thrombosis Recurrence and Survival. *Neurology* 2006, 67, 814–819. [PubMed: 16966543]
- (12). Singal AK; Kamath PS; Tefferi A Mesenteric Venous Thrombosis. *Mayo Clin. Proc.* 2013, 88, 285–294. [PubMed: 23489453]
- (13). Kesieme E; Kesieme C; Jebbin N; Irekpita E; Dongo A Deep Vein Thrombosis: a Clinical Review. *J. Blood Med.* 2011, 2, 59–69. [PubMed: 22287864]
- (14). Reichenspurner H; Navia JA; Berry G; Robbins RC; Barbut D; Gold JP; Reichart B Particulate Emboli Capture by an Intra-Aortic Filter Device during Cardiac Surgery. *J. Thorac. Cardiovasc. Surg.* 2000, 119, 233–241. [PubMed: 10649198]
- (15). Taguchi I; Kanaya T; Toi T; Abe S; Sugimura H; Hoshi T; Oida A; Araki H; Ogawa K; Kaneko N Comparison of the Effects of a Distal Embolic Protection Device and an Aspiration Catheter During Percutaneous Coronary Intervention in Patients with Acute Myocardial Infarction. *Circ. J.* 2005, 69, 49–54. [PubMed: 15635202]
- (16). Haeck JDE; Koch KT; Bilodeau L; Van der Schaaf RJ; Henriques JPS; Vis MM; Baan J; Van der Wal AC; Piek JJ; Tijssen JGP; Krucoff MW; De Winter RJ Randomized Comparison of Primary Percutaneous Coronary Intervention With Combined Proximal Embolic Protection and Thrombus Aspiration Versus Primary Percutaneous Coronary Intervention Alone in ST-Segment Elevation Myocardial Infarction. *J. Am. Coll. Cardiol. Cardiovasc. Interventions* 2009, 2, 934–943.
- (17). Kumbhani DJ; Bavry AA; Desai MY; Bangalore S; Bhatt DL Role of Aspiration and Mechanical Thrombectomy in Patients with Acute Myocardial Infarction Undergoing Primary Angioplasty: an Updated Meta-Analysis of Randomized Trials. *J. Am. Coll. Cardiol.* 2013, 62, 1409–1418. [PubMed: 23665372]
- (18). Barritt DW; Jordan SC Anticoagulant Drugs in the Treatment of Pulmonary Embolism: a Controlled Trial. *Lancet* 1960, 275, 1309–1312.

- (19). Karsch KR; Preisack MB; Baildon R; Eschenfelder V; Foley D; Garcia EJ; Kaltenbach M; Meisner C; Selbmann HK; Serruys PW; Shiu MF; Sujatta M; Bonan R Low Molecular Weight Heparin (Reviparin) in Percutaneous Transluminal Coronary Angioplasty Results of a Randomized, Double-Blind, Unfractionated Heparin and Placebo-Controlled, Multicenter Trial (REDUCE Trial). *J. Am. Coll. Cardiol.* 1996, 28, 1437–1443. [PubMed: 8917255]
- (20). Konstantinides S; Geibel A; Heusel G; Heinrich F; Kasper W; Management Strategies and Prognosis of Pulmonary Embolism-3 Trial Investigators. Heparin plus Alteplase Compared with Heparin Alone in Patients with Submassive Pulmonary Embolism. *N. Engl. J. Med.* 2002, 347, 1143–1150. [PubMed: 12374874]
- (21). Serruys PW; van Hout B; Bonnier H; Legrand V; Garcia E; Macaya C; Sousa E; van der Giessen W; Colombo A; Seabra-Gomes R; Kiemeneij F; Ruygrok P; Ormiston J; Emanuelsson H; Fajadet J; Haude M; Klugmann S; Morel MA Randomised Comparison of Implantation of Heparin-Coated Stents with Balloon Angioplasty in Selected Patients with Coronary Artery Disease (Benestent II). *Lancet* 1998, 352, 673–681. [PubMed: 9728982]
- (22). Goldhaber SZ Thrombolysis in Pulmonary Embolism: a Debatable Indication. *Thromb. Haemost.* 2001, 86, 444–451. [PubMed: 11487035]
- (23). Clark JB; Qiu F; Guan Y; Woitas KR; Myers JL; Undar A Microemboli Detection and Classification during Pediatric Cardiopulmonary Bypass. *World J. Pediatr. Congenital Heart Surg.* 2011, 2, 111–114.
- (24). Golukhova EZ; Polunina AG; Zhuravleva SV; Lefterova NP; Begachev AV Size of Left Cardiac Chambers Correlates with Cerebral Microembolic Load in Open Heart Operations. *Cardiol. Res. Prac.* 2010, 2010, 143679.
- (25). Atochin DN; Murciano JC; Gürsoy-Özdemir Y; Krasik T; Noda F; Ayata C; Dunn AK; Moskowitz MA; Huang PL; Muzykantov VR Mouse Model of Microembolic Stroke and Reperfusion. *Stroke* 2004, 35, 2177–2182.e. [PubMed: 15256680]
- (26). Nozari A; Dilekoz E; Sukhotinsky I; Stein T; Eikermann-Haerter K; Liu C; Wang Y; Frosch MP; Waeber C; Ayata C; Moskowitz MA Microemboli May Link Spreading Depression, Migraine Aura, and Patent Foramen Ovale. *Ann. Neurol.* 2010, 67, 221–229. [PubMed: 20225282]
- (27). Clark RE; Brillman J; Davis DA; Lovell MR; Price TRP; Magovern GJ Microemboli during Coronary Artery Bypass Grafting: Genesis and Effect on Outcome. *J. Thor. Cardiovasc. Surg.* 1995, 109, 249–258.
- (28). Mitchell SJ; Merry AF Perspective on Cerebral Microemboli in Cardiac Surgery: Significant Problem or Much Ado About Nothing? *J. Extracorp. Technol.* 2015, 47, 10–15.
- (29). Kruis RWJ; Vlasveld FAE; Van Dijk D The (Un)Importance of Cerebral Microemboli. *Semin. Cardiothorac. Vasc. Anesth.* 2010, 14, 111–118. [PubMed: 20478951]
- (30). Hölscher T; Raman R; Fisher DJ; Ahadi G; Zadicario E; Voie A Effects of Varying Duty Cycle and Pulse Width on High-Intensity Focused Ultrasound (HIFU)-Induced Transcranial Thrombolysis. *J. Ther. Ultrasound* 2013, 1, 18. [PubMed: 25512862]
- (31). Siegel RJ; Luo H Ultrasound Thrombolysis. *Ultrasonics* 2008, 48, 312–320. [PubMed: 18462769]
- (32). Stone MJ; Frenkel V; Dromi S; Thomas P; Lewis RP; Li KCP; Horne M; Wood BJ Pulsed-High Intensity Focused Ultrasound Enhanced TPA Mediated Thrombolysis in a Novel in Vivo Clot Model, a Pilot Study. *Thromb. Res.* 2007, 121, 193–202. [PubMed: 17481699]
- (33). Wright C; Hynynen K; Goertz D An Investigation of High Intensity Focused Ultrasound Thrombolysis. *AIP Conf. Proc.* 2011, 1359, 246–250.
- (34). Xu S; Zong Y; Feng Y; Liu R; Liu X; Hu Y; Han S; Wan M Dependence of Pulsed Focused Ultrasound Induced Thrombolysis on Duty Cycle and Cavitation Bubble Size Distribution. *Ultrason. Sonochem.* 2015, 22, 160–166. [PubMed: 25043556]
- (35). Suo D; Guo S; Lin W; Jiang X; Jing Y Thrombolysis Using Multi-Frequency High Intensity Focused Ultrasound at MHz Range: an in Vitro Study. *Phys. Med. Biol.* 2015, 60, 7403–7418. [PubMed: 26350754]
- (36). Ting Ding; Yuan Yuan; Supin Wang; Mingxi Wan. Spatial-Temporal Dynamics of Cavitation Bubbles Induced by Pulsed HIFU Thrombolysis within a Vessel and Parameters Optimization for Cavitation Enhancement. *IEEE Int. Ultrason. Symp.* 2016, 1–4.

- (37). Maxwell AD; Cain CA; Duryea AP; Yuan L; Gurm HS; Xu Z Non-Invasive Thrombolysis Using Pulsed Ultrasound Cavitation Therapy – Histotripsy. *Ultrasound Med. Biol.* 2009, 35, 1982–1994. [PubMed: 19854563]
- (38). Wright C; Hynynen K; Goertz D In Vitro and in Vivo High Intensity Focused Ultrasound Thrombolysis. *Invest. Radiol.* 2012, 47, 217–225. [PubMed: 22373533]
- (39). Lu Y; Wang J; Huang R; Chen G; Zhong L; Shen S; Zhang C; Li X; Cao S; Liao W; Liao Y; Bin J Microbubble-Mediated Sonothrombolysis Improves Outcome after Thrombotic Microembolism-Induced Acute Ischemic Stroke. *Stroke* 2016, 47, 1344–1353. [PubMed: 27048701]
- (40). Leeman JE; Kim JS; Yu FTH; Chen X; Kim K; Wang J; Chen X; Villanueva FS; Pacella JJ Effect of Acoustic Conditions on Microbubble-Mediated Microvascular Sonothrombolysis. *Ultrasound Med. Biol.* 2012, 38, 1589–1598. [PubMed: 22766112]
- (41). Xie F; Tsutsui JM; Lof J; Unger EC; Johanning J; Culp WC; Matsunaga T; Porter TR Effectiveness of Lipid Microbubbles and Ultrasound in Dec clotting Thrombosis. *Ultrasound Med. Biol.* 2005, 31, 979–985. [PubMed: 15972204]
- (42). Nishioka T; Luo H; Fishbein MC; Cercek B; Forrester JS; Kim C-J; Berglund H; Siegel RJ Dissolution of Thrombotic Arterial Occlusion by High Intensity, Low Frequency Ultrasound and Dodecafluoropentane Emulsion: An in Vitro and in Vivo Study. *J. Am. Coll. Cardiol.* 1997, 30, 561–568. [PubMed: 9247533]
- (43). Moyer LC; Timbie KF; Sheeran PS; Price RJ; Miller GW; Dayton PA High-Intensity Focused Ultrasound Ablation Enhancement in Vivo via Phase-Shift Nanodroplets Compared to Microbubbles. *J. Ther. Ultrasound* 2015, 3, 7. [PubMed: 26045964]
- (44). Mougenot C; Köhler MO; Enholm J; Quesson B; Moonen C Quantification of Near-Field Heating during Volumetric MR-HIFU Ablation. *Med. Phys.* 2011, 38, 272–282. [PubMed: 21361196]
- (45). Phillips LC; Puett C; Sheeran PS; Dayton PA; Wilson Miller G; Matsunaga TO Phase-Shift Perfluorocarbon Agents Enhance High Intensity Focused Ultrasound Thermal Delivery with Reduced Near-Field Heating. *J. Acoust. Soc. Am.* 2013, 134, 1473–1482. [PubMed: 23927187]
- (46). Rapoport N Phase-Shift, Stimuli-Responsive Perfluorocarbon Nanodroplets for Drug Delivery to Cancer. *Wiley Interdiscip. Rev. Nanomed. Nanobiotechnol.* 2012, 4, 492–510. [PubMed: 22730185]
- (47). Yildirim A; Shi D; Roy S; Blum NT; Chattaraj R; Cha JN; Goodwin AP Nanoparticle-Mediated Acoustic Cavitation Enables High Intensity Focused Ultrasound Ablation Without Tissue Heating. *ACS Appl. Mater. Interfaces* 2018, 10, 36786–36795. [PubMed: 30339360]
- (48). Yildirim A; Chattaraj R; Blum NT; Goldscheitter GM; Goodwin AP Stable Encapsulation of Air in Mesoporous Silica Nanoparticles: Fluorocarbon-Free Nanoscale Ultrasound Contrast Agents. *Adv. Healthcare Mater.* 2016, 5, 1290–1298.
- (49). Yildirim A; Chattaraj R; Blum NT; Goodwin AP Understanding Acoustic Cavitation Initiation by Porous Nanoparticles: Toward Nanoscale Agents for Ultrasound Imaging and Therapy. *Chem. Mater.* 2016, 28, 5962–5972. [PubMed: 28484307]
- (50). Pattni BS; Chupin VV; Torchilin VP New Developments in Liposomal Drug Delivery. *Chem. Rev.* 2015, 115, 10938–10966. [PubMed: 26010257]
- (51). Fricker G; Kromp T; Wendel A; Blume A; Zirkel J; Rebmann H; Setzer C; Quinkert R-O; Martin F; Müller-Goymann C Phospholipids and Lipid-Based Formulations in Oral Drug Delivery. *Pharm. Res.* 2010, 27, 1469–1486. [PubMed: 20411409]
- (52). Augustin MA; Hemar Y Nano- and Micro-Structured Assemblies for Encapsulation of Food Ingredients. *Chem. Soc. Rev.* 2009, 38, 902–912. [PubMed: 19421570]
- (53). Yildirim A; Chattaraj R; Blum NT; Shi D; Kumar K; Goodwin AP Phospholipid Capped Mesoporous Nanoparticles for Targeted High Intensity Focused Ultrasound Ablation. *Adv. Healthcare Mater.* 2017, 6, 1700514.
- (54). Blum NT; Yildirim A; Gyorkos C; Shi D; Cai A; Chattaraj R; Goodwin AP Temperature-Responsive Hydrophobic Silica Nanoparticle Ultrasound Contrast Agents Directed by Phospholipid Phase Behavior. *ACS Appl. Mater. Interfaces* 2019, 11, 15233–15240. [PubMed: 31012297]

- (55). Fowler WE; Hantgan RR; Hermans J; Erickson HP Structure of the Fibrin Protofibril. Proc. Natl. Acad. Sci. 1981, 78, 4872–4876. [PubMed: 6946434]
- (56). Vedakumari WS; Prabu P; Babu SC; Sastry TP Fibrin Nanoparticles as Possible Vehicles for Drug Delivery. Biochim. Biophys. Acta 2013, 1830, 4244–4253. [PubMed: 23643967]
- (57). Prabu P; Vedakumari WS; Sastry TP Time-Dependent Biodistribution, Clearance and Biocompatibility of Magnetic Fibrin Nanoparticles: An in Vivo Study. Nanoscale 2015, 7, 9676–9685. [PubMed: 25959634]
- (58). Duncan R; Ferruti P; Sgouras D; Tuboku-Metzger A; Ranucci E; Bignotti F A Polymer-Triton X-100 Conjugate Capable of pH-Dependent Red Blood Cell Lysis: a Model System Illustrating the Possibility of Drug Delivery Within Acidic Intracellular Compartments. J. Drug Targeting 1994, 2, 341–347.
- (59). Robles FE; Chowdhury S; Wax A Assessing Hemoglobin Concentration Using Spectroscopic Optical Coherence Tomography for Feasibility of Tissue Diagnostics. Biomed. Opt. Express 2010, 1, 310–317. [PubMed: 21258468]
- (60). Kahraman H; Ozaydin M; Varol E; Aslan SM; Dogan A; Altinbas A; Demir M; Gedikli O; Acar G; Ergene O The Diameters of the Aorta and Its Major Branches in Patients with Isolated Coronary Artery Ectasia. Tex. Heart Inst. J. 2006, 33, 463–468. [PubMed: 17215971]

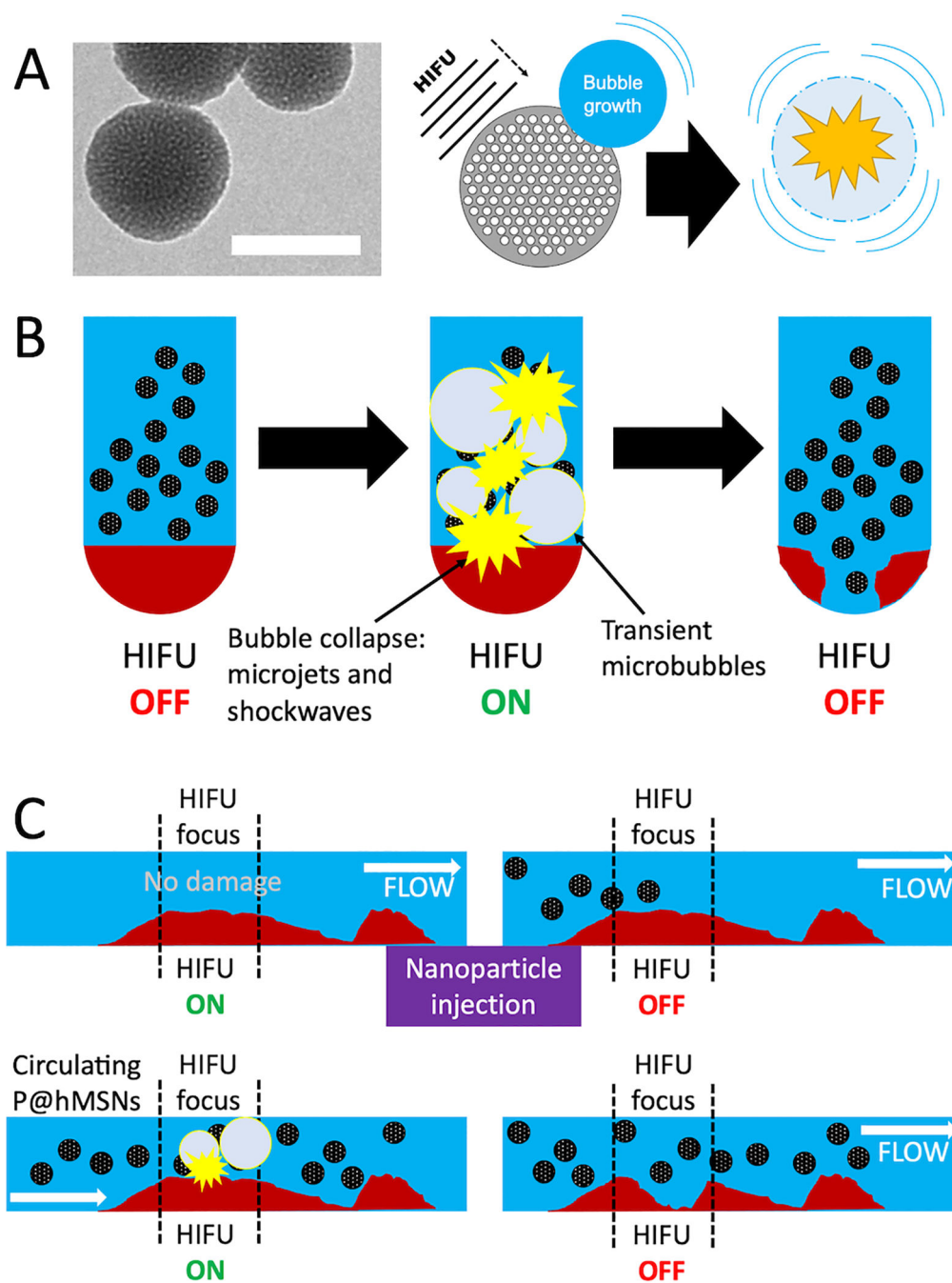


Figure 1.

A) Left: TEM images of the hMSNs; the scale bar is 100 nm. Right: Schematic showing mechanism by which P@hMSNs interact with HIFU waves to create transient cavitation events for the mechanical breakdown of the thrombus. B) Proposed mechanism by which HIFU can selectively interact with P@hMSNs in a static *in vitro* model. The HIFU waves interact with the P@hMSNs to generate transient cavitation events that break the clot down selectively in the area of HIFU focus. C) Proposed mechanism by which HIFU is assisted by P@hMSN infusion. HIFU alone does not damage the clot at baseline HIFU intensities, but

after the infusion of P@hMSNs, the sensitized cavitation events disrupt the clot mechanically in the area of HIFU focus.

Author Manuscript

Author Manuscript

Author Manuscript

Author Manuscript

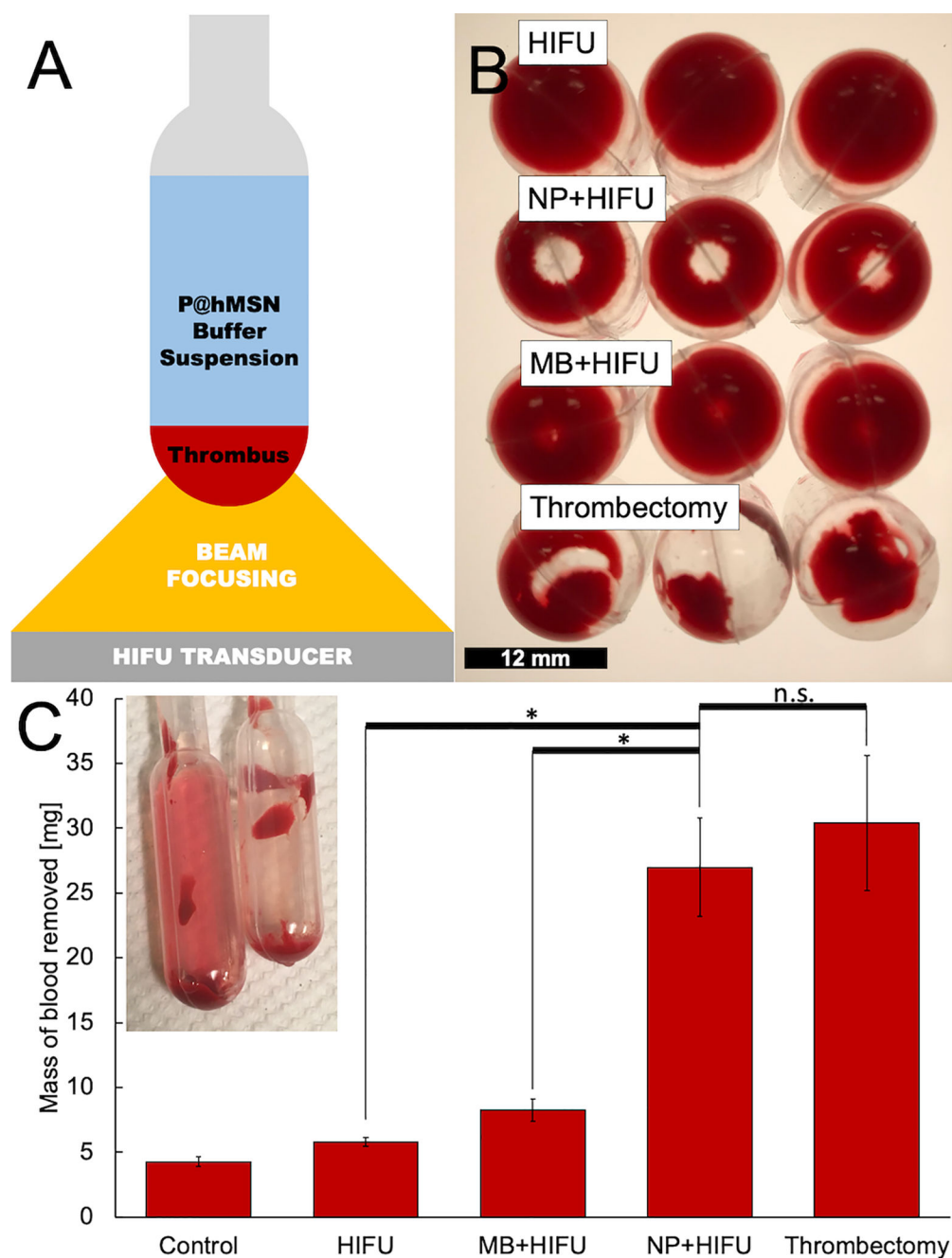


Figure 2.

A) Schematic of the experimental setup of simulated thrombus exposed to high intensity focused ultrasound (HIFU). B) Photographs of clots treated by (top to bottom): HIFU only, P@hMSNs+HIFU, Microbubbles+HIFU, and mechanical thrombectomy model. Scale bar = 12 mm. C) Mass of blood removed from a 100 μ L thrombus as determined by hemoglobin absorbance at 540 nm for four independent samples at each condition. Error bars denote one standard deviation. Inset: photograph showing (left) a HIFU+NP treated blood clot with the supernatant reddened by the disrupted thrombus, and (right) a HIFU-only control with

minimal ejection of clot matter into the buffer solution. *Indicates significant difference at $\alpha=0.05$, one-sided; n.s. denotes non-significance.

Author Manuscript

Author Manuscript

Author Manuscript

Author Manuscript

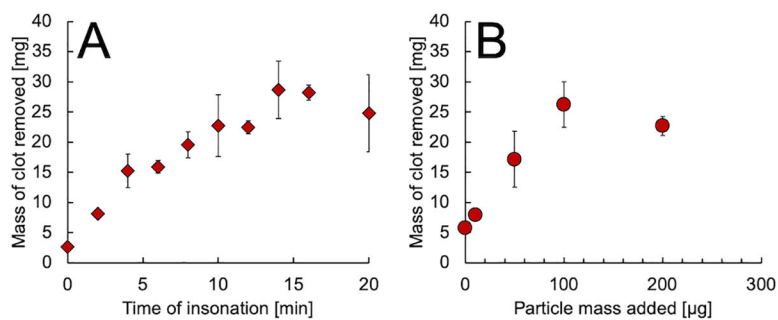
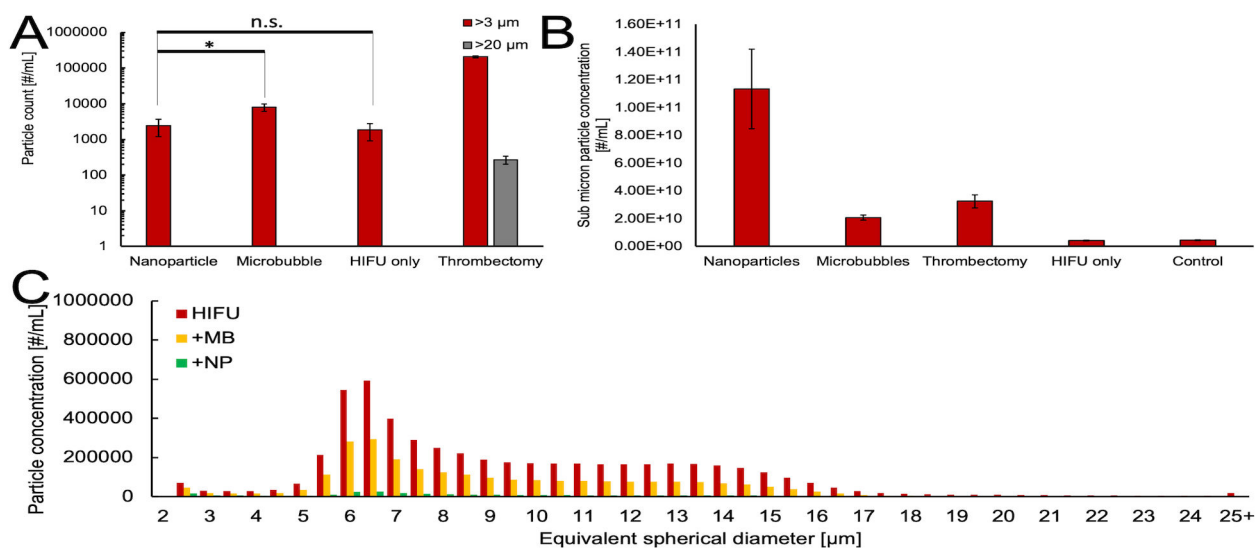


Figure 3.

A) Mass of blood released from clot vs. HIFU exposure time for clots treated with HIFU and $100 \mu\text{g mL}^{-1}$ P@hMSNs, as determined by hemoglobin absorbance at 540 nm. B) Mass of blood released from clot vs. P@hMSN mass added to the 1 mL supernatant with a constant 10 min HIFU insonation time.

**Figure 4.**

A) Counts for >3 and >20 μm equivalent spherical diameter particles from FLOWCAM imaging for each treatment. *Indicates significant difference at $\alpha=0.05$, one-sided; n.s. denotes non-significance. B) Submicron (<1 μm) particle counts as estimated from Nanoparticle Tracking Analysis, with background subtracted. The error bars correspond to one standard deviation. C) FLOWCAM particle histograms for various treatments applied to the supernatant of a thrombus after mechanical thrombectomy condition was applied. The histograms have a 0.5 μm bin size and are an amalgamation of four independently treated samples.

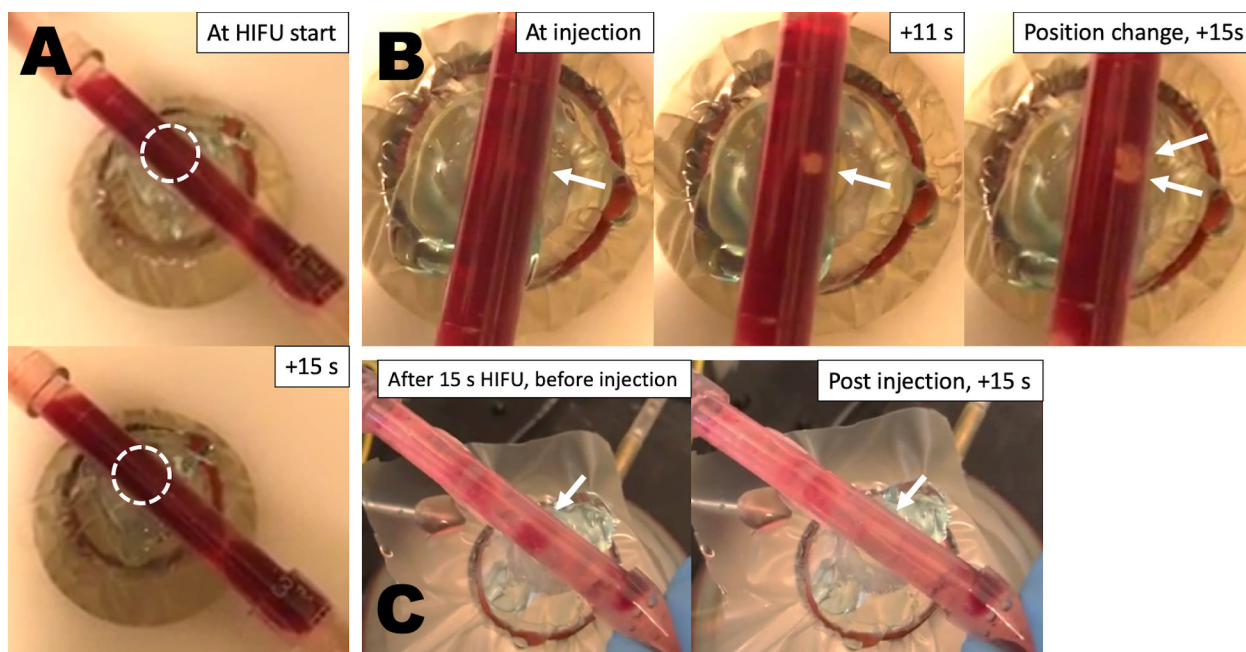


Figure 5. Still images from videos of the *in vitro* thrombolysis flow model. (A) Image of partially occlusive thrombus before and after HIFU insonation without injection of particles. (B) Images of the same blood clot at administration of P@hMSNs, then after 11 s of HIFU insonation, and once more after a position change and an additional 15 s of HIFU. (C) Another example of blood clot after 15 s of HIFU prior to P@hMSN injection, then again post injection with 15 s HIFU.